Research Article

Adaptive Dynamic Surface Control for Generator Excitation Control System

Zhang Xiu-yu,[1,2] Liu Cui-ping,[1] Wang Jian-guo,[1] and Lin Yan[2]

[1] *Northeast Dianli University, School of Automation, Jilin City, Jilin 132012, China*
[2] *Beijing University of Aeronautics and Astronautics, School of Automation, Beijing 100191, China*

Correspondence should be addressed to Zhang Xiu-yu; zhangxiuyu80@163.com

For the generator excitation control system which is equipped with static var compensator (SVC) and unknown parameters, a novel adaptive dynamic surface control scheme is proposed based on neural network and tracking error transformed function with the following features: (1) the transformation of the excitation generator model to the linear systems is omitted; (2) the prespecified performance of the tracking error can be guaranteed by combining with the tracking error transformed function; (3) the computational burden is greatly reduced by estimating the norm of the weighted vector of neural network instead of the weighted vector itself; therefore, it is more suitable for the real time control; and (4) the explosion of complicity problem inherent in the backstepping control can be eliminated. It is proved that the new scheme can make the system semiglobally uniformly ultimately bounded. Simulation results show the effectiveness of this control scheme.

1. Introduction

With the development of power system, the requirements of the load are increasing. However, the ability of the transmission network is limited and the electric power system has gradually reached its operating limit; the world power systems tend to extend power grid scale and develop larger power system. However, the power systems are more likely to encounter some problems such as oscillations and complex nonlinear phenomena due to the extension of power grid scale and some emergencies. Therefore, ways of maintaining the reliability and stability of power system are attracting more and more research interest [1–4]. Moreover, the promotion of the control ability of the generator excitation system can help us to monitor the states of system and predict system performance; it is the most effective way to improve the performance of the whole excitation control system and it has been widely of concern in recent years [5–7].

The most common method for designing generator excitation system controller is the direct-feedback-linearization, which transforms the nonlinear model into a linear one by some mathematical ways. However, it is only effective to the system when special conditions are satisfied [8, 9]. Now, more and more nonlinear control techniques are being applied to the generator excitation systems. In [10], an output feedback controller combined with high-order sliding-mode techniques is proposed to guarantee the transient stability of the power systems. In [11], for the nonlinear characteristics of the transient process in power system whose parameters are known, Colbia-Vega and his collaborators designed a controller for steam-valving and excitation system, which can stabilize the voltage and improve power quality. In [12], an adaptive fuzzy zero dynamic and sliding model control is proposed to cope with the unknown parameters, and the fuzzy logic rules are used to approximate the unknown nonlinear functions. For the time-varying and uncertainties of the reactance and voltage in one-machine infinite-bus power system, Zhang and Zhu in [13] designed an adaptive excitation controller by using strong tracking filter in the design procedure of excitation controller of generators, and the stability of the control system is improved when it is accompanied with some disturbances; however, it has the explosion of complicity problem inherent in the backstepping control. In [14], an adaptive filter control for generator excitation system was proposed based on IEEE 14-bus.
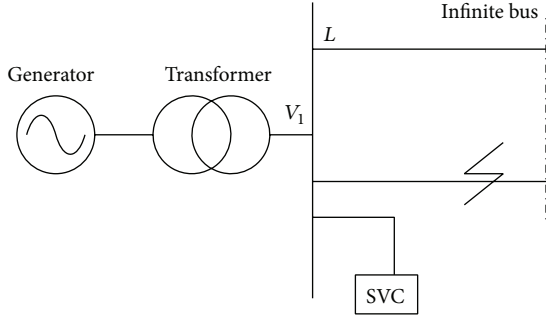
FIGURE 1: Single machine infinite bus system with SVC.

Motivated by the previous work ([12, 13], etc.) this paper has successfully fused adaptive dynamic surface control with neural network and tracking error transformed function to design a robust adaptive controller for the nonlinear power system. The features of our control scheme are as follows:

(i) the tracking error of the power angle and voltage at the SVC can be transformed to an arbitrarily prespecified performance by an error transformed function;

(ii) the neural network based adaptive dynamic surface controller is designed without doing any linearization to the excitation generator model. Therefore, the design procedures and the final control law are greatly simplified and the control accuracy is improved;

(iii) by using the neural network, the structure and the parameters of the control system can be totally unknown;

(iv) by estimating the norm of the weighted vector of neural network instead of the weighted vector itself, the computational burden is greatly reduced and it is more suitable for the real time control.

This paper is organized as follows. In Section 2, the mathematical model of excitation system of power generator is introduced and the control purpose is formulated. In Section 3, the design procedure of the neural network and the tracking error transformed function based adaptive DSC scheme is presented. Section 4 gives the stability analysis for the proposed scheme. Finally, simulation examples are given to demonstrate the effectiveness of the proposed design method.

2. The Excitation System of Power Generator

2.1. Mathematical Model. Assume that the SVC device is installed in a single-machine infinite-bus system; the structure and the equivalent circuit diagram are shown in Figure 1 [15].

To proceed, the following assumptions are made.

Assumption 1. Ignoring the dynamic process of rapid excitation equipment means the control voltage u_f is equal to the generator excitation voltage E_f, $E_f = u_f$.

Assumption 2. The mechanical power of generators remains unchanged in transient stability process; that is, $\Delta P_m = 0$.

Then, the mathematical model of the generator excitation control system equipped with SVC can be described as follows [16–18]:

$$
\begin{aligned}
\dot{\delta} &= \omega - \omega_0, \\
\dot{\omega} &= \frac{\omega_0}{H} P_{m0} - \frac{D}{H}\left(\omega - \omega_0\right) - \frac{\omega_0}{H} \frac{E_q' V_s}{X_{d\Sigma}'} \sin\delta + d_1, \\
\dot{E_q'} &= -\frac{X_{d\Sigma}}{T_{d0} X_{d\Sigma}'} E_q' + \frac{1}{T_{d0}} \frac{X_d - X_d'}{X_{d\Sigma}'} V_s \cos\delta + \frac{1}{T_{d0}} u_f + d_2, \\
\dot{B_L} &= \frac{1}{T_C}\left(-B_L + B_C + u_B\right),
\end{aligned}
\tag{1}
$$

where δ is the power angle of the generator running rotor; ω is the rotor speed of the generator (rad/s); D is the damping constant; H is the inertia constant; $\omega_0 = 2\pi f_0$ is the synchronous machine speed (rad/s); f_0 is the rated frequency (Hz); P_m is the mechanical power of motor output; T_{d0} is the direct axis transient short circuit time constant (s); T_C is the time constant of adjusting system and SVC (s); E_q' is the transient electromotive force (EMF) of the generator; $V_s = 1$ is the voltage of the system; u_f is the control voltage of excitation equipment; u_B is the input of SVC; B_L is the adjustable equivalent susceptance in SVC; B_C is the initial value of adjustable susceptance; d_1 is position bounded torque interference of the rotor; and d_2 is electromagnetic transient interference of the stator:

$$
\begin{aligned}
X_1 &= X_d' + X_T, \\
X_3 &= X_d + X_T, \\
X_{d\Sigma} &= X_3 + X_2 + X_3 X_2\left(B_L - B_C\right), \\
X_{d\Sigma}' &= X_1 + X_2 + X_1 X_2\left(B_L - B_C\right),
\end{aligned}
\tag{2}
$$

where X_2 is the transmission line reactance; X_d is the generator direct axis reactance; X_d' is the direct axis transient reactance of the generator; and X_T is the transformer reactance.

When the system encounters the external disturbances, the stability of the power angle and SVC access point voltage can be effectively improved by combining the regulation of SVC with generator-excitation adjustment. In this paper, we take increment of the power angle and accessing point voltage as the output value of the system to design our adaptive dynamic surface controller; that is,

$$
\begin{aligned}
y_1 &= \delta - \delta_0, \\
y_2 &= V_m - V_{\text{ref}},
\end{aligned}
\tag{3}
$$

where V_m is the accessing point voltage and V_{ref} is the reference voltage. According to the circuit, we have

$$V_m = \frac{\sqrt{\left(X_2 E_q'\right)^2 + \left(X_1 V_s\right)^2 + 2 X_1 X_2 E_q' V_s \cos \delta}}{X_{d\Sigma}'}. \quad (4)$$

Based on the above descriptions, let $x_1 = \delta - \delta_0$, $x_2 = \omega - \omega_0$, $x_3 = E_q'$, and $x_4 = V_m - V_{\text{ref}}$; then, (1) can be expressed as the following form:

$$\dot{x}_1 = x_2,$$

$$\dot{x}_2 = -\frac{\omega_0}{H} \frac{V_s \sin\left(x_1 + \delta_0\right)}{X_{d\Sigma}'} x_3 - \frac{D}{H} x_2$$
$$+ \frac{\omega_0}{H} P_{m0} + d_1,$$

$$\dot{x}_3 = \frac{1}{T_{d0}} u_f - \frac{X_{d\Sigma}}{T_{d0} X_{d\Sigma}'} x_3 + \frac{1}{T_{d0}} \frac{X_d - X_d'}{X_{d\Sigma}'} V_s \cos \delta + d_2,$$

$$\dot{x}_4 = -\frac{V_s \sin \delta X_1 X_2}{V_m (X_{d\Sigma}')^2} x_2 x_3 - \frac{X_1 X_2 V_m}{X_{d\Sigma}'} \cdot \frac{1}{T_c} \left(-B_L + B_C\right)$$
$$+ \frac{X_2^2 x_3 + X_1 X_2 V_s \cos \delta}{V_m (X_{d\Sigma}')^2}$$
$$\cdot \left(-\frac{X_{d\Sigma}}{T_{d0} X_{d\Sigma}'} x_3 + \frac{1}{T_{d0}} \frac{X_d - X_d'}{X_{d\Sigma}'} \cdot V_s \cos \delta\right)$$
$$+ \frac{u_f}{T_{d0} V_m (X_{d\Sigma}')^2} \cdot \left(X_2^2 x_3 + X_1 X_2 V_s \cos \delta\right)$$
$$+ \frac{X_1 X_2}{T_C X_{d\Sigma}'} \left(-x_4 u_B\right). \quad (5)$$

Let

$$g_2 = -\frac{\omega_0}{H} \frac{V_s \sin\left(x_1 + \delta_0\right)}{X_{d\Sigma}'}, \qquad g_3 = \frac{1}{T_{d0}},$$

$$g_4 = \frac{X_1 X_2}{T_C X_{d\Sigma}'}, \qquad f_2\left(\overline{x}_2\right) = -\frac{D}{H} x_2 + \frac{\omega_0}{H} P_{m0},$$

$$u_B' = -x_4 u_B,$$

$$f_4\left(\overline{x}_4\right) = -\frac{V_s \sin \delta X_1 X_2}{V_m (X_{d\Sigma}')^2} x_2 x_3 - \frac{X_1 X_2 V_m}{X_{d\Sigma}'}$$
$$\cdot \frac{1}{T_c} \left(-B_L + B_C\right) + \frac{X_2^2 x_3 + X_1 X_2 V_s \cos \delta}{V_m (X_{d\Sigma}')^2} \quad (6)$$
$$\cdot \left(-\frac{X_{d\Sigma}}{T_{d0} X_{d\Sigma}'} x_3 + \frac{1}{T_{d0}} \cdot \frac{X_d - X_d'}{X_{d\Sigma}'} V_s \cos \delta\right)$$
$$+ \frac{X_2^2 x_3 + X_1 X_2 V_s \cos \delta}{T_{d0} V_m (X_{d\Sigma}')^2} u_f,$$

$$f_3\left(\overline{x}_3\right) = -\frac{X_{d\Sigma}}{T_{d0} X_{d\Sigma}'} x_3 + \frac{1}{T_{d0}} \frac{X_d - X_d'}{X_{d\Sigma}'} V_s \cos \delta,$$

where $\overline{x}_i := [x_1, \ldots, x_i]^T \in R^i$, $i = 1, \ldots, 4$, are state vectors. Then, the system (5) can be converted into the following two independent subsystems (7) and (8), whose relative degree is 3 and 1, respectively:

$$\dot{x}_1 = x_2,$$

$$\dot{x}_2 = g_2 x_3 + f_2\left(\overline{x}_2\right) + d_1,$$

$$\dot{x}_3 = g_3 u_f + f_3\left(\overline{x}_3\right) + d_2, \quad (7)$$

$$y_1 = x_1,$$

$$\dot{x}_4 = g_4 u_B' + f_4\left(\overline{x}_4\right),$$

$$y_2 = x_4. \quad (8)$$

Now, we can design our adaptive dynamic surface control law of the power system based on the following assumptions.

Assumption 3. The value of g_2 is unknown but the sign of g_2 is known; it is assumed that there exist two constants g_m and $g_{2\max}$ satisfying

$$0 < g_m \leq |g_2| \leq g_{2\max}. \quad (9)$$

Assumption 4. The reference signal y_r is smooth and bounded; $[y_r, \dot{y}_r, \ddot{y}_r]^T$ belong to a compact set for all $t \geq 0$.

Remark 5. Assumptions 1 and 2 which are the same as those in [15] are used to construct the model of the excitation system of power generator. Assumption 3 is used in Section 4, such as in the proof of (59), (65), and (67). We also emphasize that g_m and $g_{2\max}$ are not required in the implementation of our control law but are required for analysis only. Assumption 4 is common in all dynamic surface control schemes.

2.2. RBF Neural Network. In general, the neural network is a multi-input single-output system [19]; the mathematical expression is

$$Y = \vartheta^T \psi\left(\xi\right), \quad (10)$$

where $\xi \in \mathbb{R}^n$ is the input of RBF neural network; $Y \in \mathbb{R}$ is the output of RBFNN, $\vartheta \in \mathbb{R}^N$ is an N-dimensional parameter vector, and here N is the number of neurons; $\psi(\xi) : \mathbb{R}^n \to \mathbb{R}^N$ is nonlinear vector function and $\psi(\xi) = [\psi_1(\xi), \ldots, \psi_N(\xi)]^T$ and $\psi_k(\xi)$ is the Gauss function.

Lemma 6. *RBFNN is a universal approximator in the sense that, given any real continuous function $\mathcal{F}(\cdot) : \Omega_\xi \to \mathbb{R}$ with $\Omega_\xi \subseteq \mathbb{R}^n$ a compact set and any $\delta_m > 0$, by appropriately choosing σ_k and ζ_k, $k = 1, \ldots, N$, for some sufficiently large integer N, there exists an RBF network [20], $\forall \xi \in \Omega_\xi \subseteq \mathbb{R}^n$, $|\delta| \leq \delta_m$,*

$$\mathcal{F}\left(\xi\right) = \vartheta^{*T} \psi\left(\xi\right) + \delta\left(\xi\right), \quad (11)$$

where ϑ^* is the optimal weight vector of ϑ and $\delta(\xi)$ is approximation error and can be defined as

$$\vartheta^* = \arg\min_{\vartheta \in \mathbb{R}^n} \left\{ \sup_{\xi \in \Omega_\xi} |Y(\xi) - \mathcal{F}(\xi)| \right\}, \tag{12}$$

$$\delta(\xi) = \mathcal{F}(\xi) - \vartheta^{*T}\psi(\xi). \tag{}$$

2.3. Error Transformed Function. We define the tracking error:

$$e := y - y_r, \tag{13}$$

where y_r is the desired trajectory. According to [21, 22], the performance function and error transformed function are defined as follows: a performance function $\varpi(t) : \mathbb{R}_+ \to \mathbb{R}_- - \{0\}$ is defined as a positive smooth decreasing function, such that, for all $t \geq 0$,

$$\begin{aligned} -\sigma\varpi(t) < e(t) < \varpi(t), & \quad \text{if } e(0) > 0, \\ -\varpi(t) < e(t) < \sigma\varpi(t), & \quad \text{if } e(0) < 0, \end{aligned} \tag{14}$$

where $0 < \sigma < 1$ and $\lim_{t \to \infty} = \varpi_\infty > 0$ and ϖ_∞ is the maximum allowable tracking error of steady-state. To convert (14) into an equivalent unconstrained one, define the error transformed function

$$e(t) := \varpi(t)\Phi(S_1), \tag{15}$$

where S_1 is the transformed error and $\Phi(S_1)$ is a smooth and strictly monotone increasing function; the inverse function has the following properties:

$$\begin{aligned} -\sigma < \Phi(S_1) < 1, & \quad \text{if } e(0) > 0, \\ -1 < \Phi(S_1) < \sigma, & \quad \text{if } e(0) < 0, \end{aligned} \tag{16}$$

where

$$\begin{aligned} \lim_{S_1 \to -\infty} \Phi(S_1) = -\sigma, & \quad \lim_{S_1 \to \infty} \Phi(S_1) = 1, & \quad \text{if } e(0) > 0, \\ \lim_{S_1 \to -\infty} \Phi(S_1) = -1, & \quad \lim_{S_1 \to \infty} \Phi(S_1) = \sigma, & \quad \text{if } e(0) < 0. \end{aligned} \tag{17}$$

As (17) shows, if $S_1 \in \mathscr{L}_\infty$, (16) holds. Take $\varpi(t) > 0$ and (15) into consideration, and we can have $-\sigma\varpi(t) < \varpi(t)\Phi(S_1) < 1$ (if $e(0) > 0$) or $-\varpi(t) < \varpi(t)\Phi(S_1) < \sigma\varpi(t)$ (if $e(0) < 0$); that is, (14) holds. Hence, from the above analysis, to achieve the prespecified tracking performance, we just only need to show that $S_1 \in \mathscr{L}_\infty$, where the strictly increasing property of $\Phi(S_1)$ guarantees that we can obtain

$$S_1 = \Phi^{-1}\left(\frac{e(t)}{\varpi(t)}\right). \tag{18}$$

Note that the case $e(0) = 0$ can be incorporated into $e(0) > 0$ or $e(0) < 0$. At the same time, σ cannot be chosen to be zero due to $S_1(0)$ being infinite.

3. Adaptive Dynamic Surface Control of Generator Excitation System

According to the mathematical model of the generator excitation system that is shown in (7), we design adaptive dynamic surface controller about power angle subsystem as follows.

Step 1. Let the first surface error and the tracking error as (18) be defined:

$$\begin{aligned} \dot{S}_1 &= \Psi\left[-\frac{\dot{\varpi}}{\varpi}e + x_2 - \dot{y}_r\right], \\ \Psi &:= \frac{1}{\varpi}\frac{\partial \Phi^{-1}}{\partial(e/\varpi)}, \end{aligned} \tag{19}$$

where y_r is an ideal output of the power angle; we suppose that y_r is a smooth and continuous function, $e := y_1 - y_r = x_1 - y_r$.

Consider the following quadratic function:

$$V_1 = \frac{1}{2}S_1^2. \tag{20}$$

We can obtain that

$$\dot{V}_1 = S_1\left[\Psi\left(-\frac{\dot{\varpi}}{\varpi}e - \dot{y}_r\right) + \Psi(x_2 - x_{2d}) + \Psi x_{2d}\right], \tag{21}$$

where x_{2d} is the virtual control signal that will be designed; choose the virtual control law as follows to stabilize (21):

$$x_{2d} = \frac{\left[-k_1 S_1 - \Psi\left(-(\dot{\varpi}/\varpi)e + \Psi S_1 - \dot{y}_r\right)\right]}{\Psi}. \tag{22}$$

In order to avoid "differential explosion," the new variable z_2 is obtained by first-order low pass filter:

$$\tau_2 \dot{z}_2 + z_2 = x_{2d}, \tag{23}$$

where τ_2 is the filter time constant.

Step 2. Define the second surface error:

$$S_2 = x_2 - z_2. \tag{24}$$

Consider the following quadratic function:

$$V_2 = \frac{1}{2}\left(S_2^2 + \frac{g_m}{\gamma_{v_2}}\tilde{v}_2^2\right). \tag{25}$$

The time derivative of V_2 is

$$\dot{V}_2 = S_2\left[g_2 x_3 + f_2(\bar{x}_2) + d_1 - \dot{z}_2\right] + \frac{g_m}{\gamma_{v_2}}\tilde{v}_2\dot{\tilde{v}}_2. \tag{26}$$

We need to use neural network to approximate the unknown terms on a compact set Ω_{ξ_2}:

$$\frac{1}{g_2}\left[f_2(\bar{x}_2) - \dot{z}_2 + d_1 + \frac{3}{2}g_2^2 S_2\right] = \theta_{\delta_2}^{*T}\psi_2(\xi_2) + \delta_2^*(\xi_2), \tag{27}$$

where $\xi_2 := (x_1, x_2, x_{2d}, z_2) \in \Omega_{\xi_2} \subset \mathbb{R}^4$; define $\widetilde{v}_2 = \widehat{v}_2 - v_2^*$, and γ_{v_2} is a positive design parameter. Let the estimated value of $v_2^* = (1/g_m)\|\theta_{\delta_2}^{*T}\|^2$ be $\widehat{v}_2$, according to inequality

$$g_2 S_2 \theta_{\delta_2}^{*T} \psi_2 \leq \frac{g_m \alpha_2^2 S_2^2 v_2^* \psi_2^T \psi_2}{2} + \frac{g_{2\max}^2}{2\alpha_2^2}, \tag{28}$$

$$g_2 S_2 \delta_2 \leq \frac{1}{2} g_2^2 S_2^2 + \frac{1}{2} \delta_2^{*2}(\xi_2). \tag{29}$$

From (27) and (28), we have

$$\dot{V}_2 \leq S_2 \left[g_2 (x_3 - x_{3d}) + g_2 x_{3d} + \frac{g_m \alpha_2^2 S_2 v_2^* \psi_2^T \psi_2}{2} \right] \tag{30}$$

$$- g_2^2 S_2^2 + \frac{1}{2} \delta_2^{*2} + \frac{g_{2\max}^2}{2\alpha_2^2} + \frac{g_m}{\gamma_{v_2}} \widetilde{v}_2 \dot{\widehat{v}}_2,$$

where x_{3d} is the virtual control signal to be designed; let the power angle actual control law and parameter adjustment law, respectively, be as follows:

$$x_{3d} = \text{sgn}(g_2) \left(-k_2 S_2 - \frac{\alpha_2^2 S_2 \widehat{v}_2 \psi_2^T \psi_2}{2} \right), \tag{31}$$

$$\dot{\widehat{v}}_2 = \gamma_{v_2} \left[\frac{\alpha_2^2 S_2^2 \psi_2^T \psi_2}{2} - \sigma_{v_2} \widehat{v}_2 \right]. \tag{32}$$

The new variable z_3 is obtained by first-order low pass filter:

$$\tau_3 \dot{z}_3 + z_3 = x_{3d}, \tag{33}$$

where τ_3 is the filter time constant. In order to avoid "differential explosion" problem brought by backstepping control, we use z_3 instead of x_{3d} in the following.

Step 3. Define the third surface error:

$$S_3 = x_3 - z_3. \tag{34}$$

Consider the following quadratic function:

$$V_3 = \frac{1}{2} \left(\frac{1}{g_3} S_3^2 + \frac{1}{\gamma_{v_3}} \widetilde{v}_3^2 \right). \tag{35}$$

The time derivative of V_3 is

$$\dot{V}_3 = S_3 \left[u_f + \frac{f_3(\overline{x}_3)}{g_3} + \frac{d_2}{g_3} - \frac{\dot{z}_3}{g_3} \right] + \frac{1}{\gamma_{v_3}} \widetilde{v}_3 \dot{\widehat{v}}_3. \tag{36}$$

Similar to second step, we use neural network to approximate the unknown term in a compact set:

$$\frac{1}{g_3} \left[f_3(\overline{x}_3) - \dot{z}_3 + d_2 \right] = \theta_{\delta_3}^{*T} \psi_3(\xi_3) + \delta_2^*(\xi_3), \tag{37}$$

where $\xi_3 := (x_1, x_2, x_3, x_{3d}, z_3) \in \Omega_{\xi_3} \subset \mathbb{R}^5$; let $\widetilde{v}_3 = \widehat{v}_3 - v_3^*$, γ_{v_3} is positive design parameter, and $\widehat{v}_3$ is the estimate value of $v_3^* = \|\theta_{\delta_3}^{*T}\|^2$. Consider the hypothesis; we have

$$\dot{V}_3 \leq S_3 \left[u_f + \frac{\alpha_3^2 S_3 v_3^* \psi_3^T \psi_3}{2} + \frac{S_3}{2} \right] \tag{38}$$

$$+ \frac{1}{2} \delta_3^{*2}(\xi_3) + \frac{1}{2\alpha_3^2} + \frac{1}{\gamma_{v_3}} \widetilde{v}_3 \dot{\widehat{v}}_3.$$

Let the power angle actual control law and parameter adjustment law be, respectively, as follows:

$$u_f = -k_3 S_3 - \frac{\alpha_3^2 S_3 \widehat{v}_3 \psi_3^T \psi_3}{2} - \frac{S_3}{2}, \tag{39}$$

$$\dot{\widehat{v}}_3 = \gamma_{v_3} \left[\frac{\alpha_3^2 S_3^2 \psi_3^T \psi_3}{2} - \sigma_{v_3} \widehat{v}_3 \right]. \tag{40}$$

Similarly, we design controller for the voltage subsystem (8); surface error is defined in (18):

$$\dot{S}_4 = \Psi_2 \left[-\frac{\dot{\omega}_2}{\omega_2} e_2 + g_4 u_B' + f_4(\overline{x}_4) - \dot{y}_{r2} \right], \tag{41}$$

$$\Psi_2 := \frac{1}{\omega_2} \frac{\partial \Phi^{-1}}{\partial (e_2/\omega_2)},$$

where $e_2 := y_2 - y_{r2} = x_4 - y_{r2}$, y_{r2} is the ideal voltage reference signal; consider the following quadratic function:

$$V_4 = \frac{1}{2} \left(\frac{1}{g_4} S_4^2 + \frac{1}{\gamma_{v_4}} \widetilde{v}_4^2 \right). \tag{42}$$

The time derivative of V_4 is

$$\dot{V}_4 = S_4 \left[\frac{\Psi_2}{g_4} \left(-\frac{\dot{\omega}_2}{\omega_2} e_2 - \dot{y}_{r2} \right) + \frac{\Psi_2 f_4(\overline{x}_4)}{g_4} + \Psi_2 u_B' \right] \tag{43}$$

$$+ \frac{1}{\gamma_{v_4}} \widetilde{v}_4 \dot{\widehat{v}}_4.$$

We use neural network to approximate $f_4(\overline{x}_4)$:

$$\frac{1}{g_4} \Psi_2 \left[f_4(\overline{x}_4) - \frac{\dot{\omega}_2}{\omega_2} e_2 - \dot{y}_{r2} \right] = \theta_{\delta_4}^{*T} \psi_4(\xi_4) + \delta_4^*(\xi_4), \tag{44}$$

where $\xi_4 := (x_4, \omega_2, \dot{\omega}_2, e_2, \dot{y}_{r2}) \in \Omega_{\xi_4} \subset \mathbb{R}^5$; let $\widetilde{v}_4 = \widehat{v}_4 - v_4^*$, γ_{v_3} is a positive design parameter, and $\widehat{v}_4$ is an estimate value of $v_4^* = \|\theta_{\delta_4}^{*T}\|^2$:

$$\dot{V}_4 \leq S_4 \left[\frac{\alpha_4^2 S_4 v_4^* \psi_4^T \psi_4}{2} + \Psi_2 u_B' + \frac{1}{2} S_4 \right] \tag{45}$$

$$+ \frac{1}{2} \delta_4^{*2}(\xi_4) + \frac{1}{2\alpha_4^2} + \frac{1}{\gamma_{v_4}} \widetilde{v}_4 \dot{\widehat{v}}_4.$$

Design voltage control law and parameter adjustment law are, respectively, as follows:

$$u_B' = \frac{1}{\Psi_2} \left[-k_4 S_4 - \frac{1}{2} S_4 - \frac{\alpha_4^2 S_4 \widehat{v}_4 \psi_4^T \psi_4}{2} \right], \tag{46}$$

$$\dot{\widehat{v}}_4 = \gamma_{v_4} \left[\frac{\alpha_4^2 S_4^2 \psi_4^T \psi_4}{2} - \sigma_{v_4} \widehat{v}_4 \right].$$

Remark 7. We emphasize our dynamic surface control scheme which, combined with tracking error transformed function (15), is also suitable for the half-car active suspension system that is described in [23, 24].

4. Stability Analysis

This section will conduct stability analysis for dynamic surface control scheme on the generator excitation system. Although the control law is simple, the stability analysis is relatively complex due to the introduction of first-order low-pass filters. For the first subsystem in (7), to begin with, we define

$$
\begin{aligned}
y_{e2} &= z_2 - x_{2d} \\
&= z_2 + \frac{[k_1 S_1 + \Psi(-(\dot{\omega}/\omega)e + \Psi S_1 - \dot{y}_r)]}{\Psi},
\end{aligned} \tag{47}
$$

$$
y_{e3} = z_3 - x_{3d} = z_3 \pm \left(k_2 S_2 + \frac{\alpha_2^2 S_2 \hat{v}_2 \psi_2^T \psi_2}{2} \right), \tag{48}
$$

where x_{2d} and x_{3d} are designed in (22) and (31), respectively. From (23) and (33), we have

$$
\begin{aligned}
\dot{z}_2 &= \frac{(x_{2d} - z_2)}{\tau_2} = -\frac{y_{e2}}{\tau_2}, \\
\dot{z}_3 &= \frac{(x_{3d} - z_3)}{\tau_3} = -\frac{y_{e3}}{\tau_3}.
\end{aligned} \tag{49}
$$

Then, the time derivative of (47) and (48) is

$$
\begin{aligned}
\dot{y}_{e2} &= -\frac{y_{e2}}{\tau_2} + \frac{k_1 \dot{S}_1}{\Psi} + \frac{k_1 S_1 \dot{\Psi}}{\Psi^2} + \left(\frac{\ddot{\omega}}{\omega} e - \frac{\dot{\omega}^2}{\omega^2} e + \frac{\dot{\omega}}{\omega} \dot{e} \right) \\
&\quad + \left(\dot{\Psi} S_1 + \Psi \dot{S}_1 \right) - \ddot{y}_r \\
&= -\frac{y_{e2}}{\tau_2} + B_2 \left(S_1, S_2, y_2, \omega, \dot{\omega}, \ddot{\omega}, y_r, \dot{y}_r, \ddot{y}_r \right), \\
\dot{y}_{e3} &= -\frac{y_{e3}}{\tau_3} \pm \left[k_2 \dot{S}_2 + \frac{\alpha_2^2 \dot{S}_2 \hat{v}_2 \psi_2^T \psi_2}{2} + \frac{\alpha_2^2 S_2 \dot{\hat{v}}_2 \psi_2^T \psi_2}{2} \right. \\
&\quad \left. + \alpha_2^2 S_2 \dot{\hat{v}}_2 \psi_2 \times \left(\sum_{j=1}^2 \frac{\partial \psi_2}{\partial x_j} \dot{x}_j + \frac{\partial \psi_2}{\partial S_2} \right) \right] \\
&= -\frac{y_{e3}}{\tau_3} + B_3 \left(S_1, S_2, S_3, y_2, y_3, \hat{v}_2, \omega, \dot{\omega}, \ddot{\omega}, y_r, \dot{y}_r, \ddot{y}_r \right),
\end{aligned} \tag{50}
$$

where B_2 and B_3 are continuous functions.

Theorem 8. *Consider the closed-loop control system composed by object (7), first-order low-pass filter (23), (33), the actual control law (39), and parameter adjustment law (40):*

$$
V = V_1 + V_2 + V_3 + \frac{1}{2} y_{e2}^2 + \frac{1}{2} y_{e3}^3, \tag{51}
$$

where V_1, V_2, and V_3, respectively, are defined by (20), (25), and (35). We suppose that for the given positive constant δ_i^*, (27), (37), and (44) meet $|\delta_i(\xi_i)| \le \delta_i^*$, $i = 2, 3, 4$, in a compact set. For any given positive parameter p, if

$$
V(0) \le p, \tag{52}
$$

then through the proper selection of the design parameters k_1, k_2, k_3, $\gamma_{v_2}, \gamma_{v_3}$, σ_{v_2}, and σ_{v_3} all the variables in the closed-loop system are uniformly ultimately bounded. The tracking performance of the system can be specified in advance.

Proof. The derivative of V by considering (51) is

$$
\dot{V} = \dot{V}_1 + \dot{V}_2 + \dot{V}_3 + y_{e2} \dot{y}_{e2} + y_{e3} \dot{y}_{e3}. \tag{53}
$$

From (24) and (47), we have

$$
x_2 = S_2 + y_{e2} + x_{2d}. \tag{54}
$$

And consider the inequality

$$
\begin{aligned}
\Psi S_1 S_2 &\le \frac{1}{2} \Psi^2 S_1^2 + \frac{1}{2} S_2^2, \\
\Psi S_1 y_{e2} &\le \frac{1}{2} \Psi^2 S_1^2 + \frac{1}{2} y_{e2}^2.
\end{aligned} \tag{55}
$$

Substituting (54) and (55) and virtual control law (22) into (21), we have

$$
\dot{V}_1 \le -k_1 S_1^2 + \frac{1}{2} S_2^2 + \frac{1}{2} y_{e2}^2. \tag{56}
$$

Using (34) and (48),

$$
x_3 = S_3 + y_{e3} + x_{3d}. \tag{57}
$$

At the same time,

$$
\begin{aligned}
g_2 S_2 S_3 &\le \frac{1}{2} g_2^2 S_2^2 + \frac{1}{2} S_3^2, \\
g_2 S_2 y_{e3} &\le \frac{1}{2} g_2^2 S_2^2 + \frac{1}{2} y_{e3}^2.
\end{aligned} \tag{58}
$$

Substitute (57) and (58), virtual control law (31), and parameter adjustment law (32) into (30):

$$
\begin{aligned}
\dot{V}_2 &\le -k_2 |g_2| S_2^2 + \frac{1}{2} S_3^2 + \frac{1}{2} y_{e3}^2 \\
&\quad + \frac{1}{2} \delta_2^{*2} + \frac{g_{2\max}^2}{2\alpha_2^2} - g_m \sigma_{v_2} \hat{v}_2 \tilde{v}_2.
\end{aligned} \tag{59}
$$

From (39) and (40), (38) can be transformed as

$$
\dot{V}_3 \le -k_3 S_3^2 + \frac{1}{2} \delta_3^{*2} + \frac{1}{2\alpha_3^2} - \sigma_{v_3} \hat{v}_3 \tilde{v}_3. \tag{60}
$$

According to Assumption 4,

$$
\Pi := \left\{ (y_r, \dot{y}_r, \ddot{y}_r) : y_r^2 + \dot{y}_r^2 + \ddot{y}_r \le B_0 \right\} \tag{61}
$$

is a compact set in $\mathbb{R}^3$, and $B_0 > 0$. M_2 is the maximum of $|B_2|$ in Π; M_3 is the maximum of $|B_3|$ at Π. For any $p > 0$, using inequality, we can obtain that

$$
|y_{e2} B_2| \le \frac{y_{e2}^2 B_2^2}{2\mu} + \frac{\mu}{2} \le \frac{y_{e2}^2 M_2^2}{2\mu} + \frac{\mu}{2}, \tag{62}
$$

$$
|y_{e3} B_3| \le \frac{y_{e3}^2 B_3^2}{2\mu} + \frac{\mu}{2} \le \frac{y_{e3}^2 M_3^2}{2\mu} + \frac{\mu}{2}, \tag{63}
$$

where μ is a positive constant parameter

$$\frac{1}{\tau_2} = \frac{1}{2} + \frac{M_2^2}{2\mu} + \alpha_0,$$

$$\frac{1}{\tau_3} = \frac{1}{2} + \frac{M_3^2}{2\mu} + \alpha_0. \tag{64}$$

Furthermore,

$$-g_m\sigma_{v_2}\widehat{v}_2\widetilde{v}_2 \le -\frac{\sigma_{v_2}g_m}{2}\widetilde{v}_2^2 + \frac{\sigma_{v_2}g_m}{2}v_2^{*2}, \tag{65}$$

$$-\sigma_{v_3}\widehat{v}_3\widetilde{v}_3 \le -\frac{\sigma_{v_3}}{2}\widetilde{v}_3^2 + \frac{\sigma_{v_3}}{2}v_3^{*2}. \tag{66}$$

Taking (56), (59), (60), and (62)–(66) into consideration, (53) can be transformed into the following equation:

$$\dot{V} \le -k_1 S_1^2 - \left(k_2 g_m - \frac{1}{2}\right)S_2^2 - \left(k_3 - \frac{1}{2}\right)S_3^2$$
$$- \alpha_0 y_{e2}^2 - \alpha_0 y_{e3}^2 - \frac{\sigma_{v_2}g_m}{2}\widetilde{v}_2^2 - \frac{\sigma_{v_3}}{2}\widetilde{v}_3^2 + C, \tag{67}$$

where

$$C = \frac{\sigma_{v_2}g_m}{2}v_2^{*2} + \frac{\sigma_{v_3}}{2}v_3^{*2} + \mu + \frac{1}{2}\delta_2^{*2}$$
$$+ \frac{1}{2}\delta_3^{*2} + \frac{g_{2\max}^2}{2\alpha_2^2} + \frac{1}{2\alpha_3^2}. \tag{68}$$

And α_0 is a positive design parameter:

$$\alpha_0 \le \min\left\{k_1, k_2 g_m - \frac{1}{2}, k_3 - \frac{1}{2}, \frac{\gamma_{v_2}\sigma_{v_2}}{2}, \frac{\gamma_{v_3}\sigma_{v_3}}{2}\right\}. \tag{69}$$

From (67), we have

$$\dot{V} \le -2\alpha_0 V + C. \tag{70}$$

Let

$$\alpha_0 > \frac{C}{2p}. \tag{71}$$

We can see that when $V = p$, $\dot{V} \le 0$. So, $V \le p$ is an invariant set. If $V(0) \le p$, then, for all $t \ge 0$, $V(t) \le p$. From (70), $\forall t \ge 0$,

$$0 \le V(t) \le \frac{C}{2\alpha_0} + \left\{V(0) - \frac{C}{2\alpha_0}\right\}e^{-2\alpha_0 t}. \tag{72}$$

Then,

$$\lim_{t \to \infty} V(t) = \frac{C}{2\alpha_0}. \tag{73}$$

Similar to the second subsystems, we substitute (46) into (45):

$$\dot{V}_4 \le -k_4 S_4^2 - \frac{\sigma_{v_4}}{2}\widetilde{v}_4^2 + \frac{1}{2}\delta_4^{*2} + \frac{1}{2\alpha_4^2} + \frac{\sigma_{v_4}}{2}v_4^{*2}. \tag{74}$$

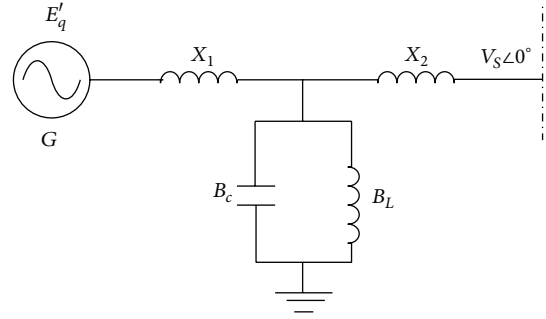Figure 2: The equivalent circuit diagram.

Let

$$k_4 \ge \frac{a}{g_4}, \tag{75}$$

$$\sigma_{v_4} \ge \frac{2a}{\gamma_{v_4}}, \tag{76}$$

$$C_2 = \frac{\sigma_{v_4}}{2}v_4^{*2} + \frac{1}{2}\delta_4^{*2} + \frac{1}{2\alpha_4^2}. \tag{77}$$

We have

$$\dot{V}_4 \le -2aV + C_2, \tag{78}$$

$$\lim_{t \to \infty} V_4(t) = \frac{C}{2a}. \tag{79}$$

As a result, all the signals such as S_1, S_2, S_3, S_4, k_1, k_2, k_3, k_4, σ_{v_2}, σ_{v_3}, σ_{v_4}, α_0, and a in the closed-loop system are uniformly bounded. In addition, (69), (75), and (76) show that, by selecting appropriate design parameters, α_0, a can be infinite; (73) and (79) show that the tracking error can converge to an arbitrary small value. □

5. Simulation Analysis

The single machine infinite bus power system with SVC is shown in Figures 1 and 2, assuming that the amplitude and frequency of receiving end bus voltage are not changed.

System parameters are $X_d' = 0.344$, $X_d = 0.982$, $X_T = 0.1$, $D = 2$, $X_{d\Sigma}' = 0.6967$, $B_L = 1.55$, $B_C = 0.5$, $T_{d0} = 5$, $T_C = 2$, $H = 13$, $E_q' = 1.059$, $\delta_0 = 40$, $\omega_0 = 100\pi$ rad/s, $P_{m0} = 1$, $V_s = 1$, $V_{ref} = 1$, $X_2 = 0.35$, and $X_{d\Sigma} = 1.4$.

In the simulation the initial values of the states are $x_1(0) = 40$, $x_2(0) = 100\pi$, $x_3(0) = 1.05$, and $x_3(0) = 1$. For NN Gaussian function $\psi_j(\xi_i) = \exp[-(\xi_i - \zeta_j)^T(\xi_i - \zeta_j)/\eta_j^2]$, $i = 2, 3, 4$, we choose 21 nodes with the centers of the basis functions ζ_j evenly spaced in $[-40, +40] \times [-314, +3144] \times [-2, +2] \times [-1, +1]$ and width $\eta_j = 1$, for $j = 1, \ldots, 21$. Also, we choose a smooth and strictly monotone increasing function, $\Phi_2(S_4) = (2/\pi)\arctan(S_4)$, $\varpi(t) = 0.65e^{-8t} + 0.002$ and $S_4 = \tan((\pi/2)\cdot(e_2(t)/\overline{w}_2(t)))$, which means that $\Psi_2 = (\pi/2)\cdot(1/\varpi_2)\cdot\cos^{-2}((\pi/2)\cdot(e_2/\varpi_2))$.
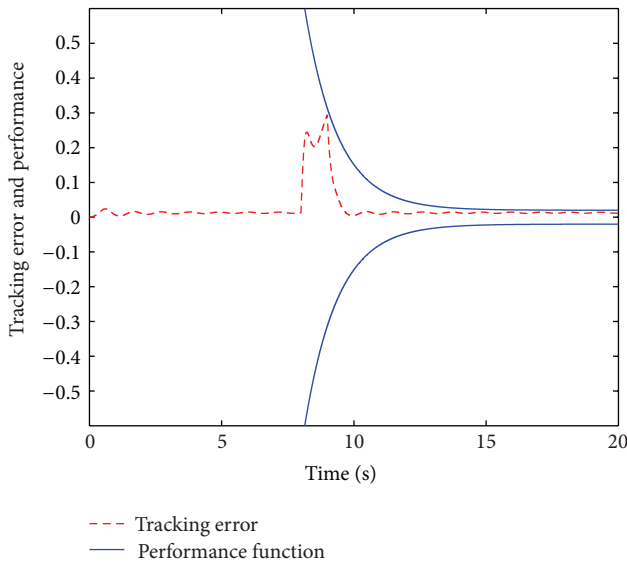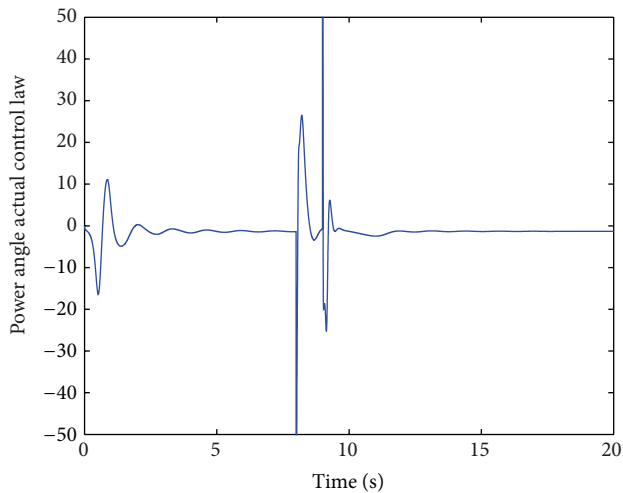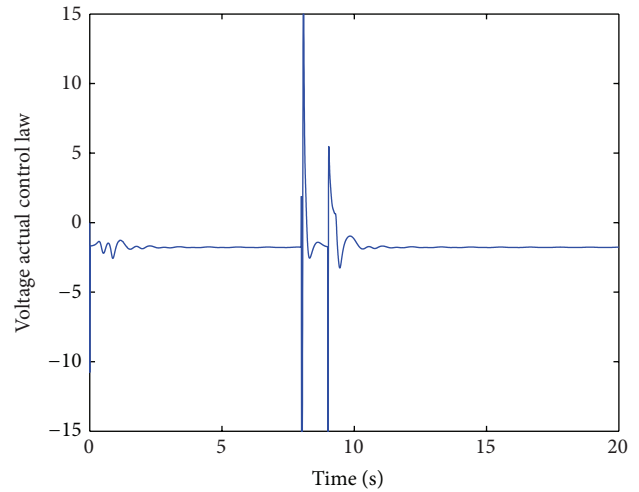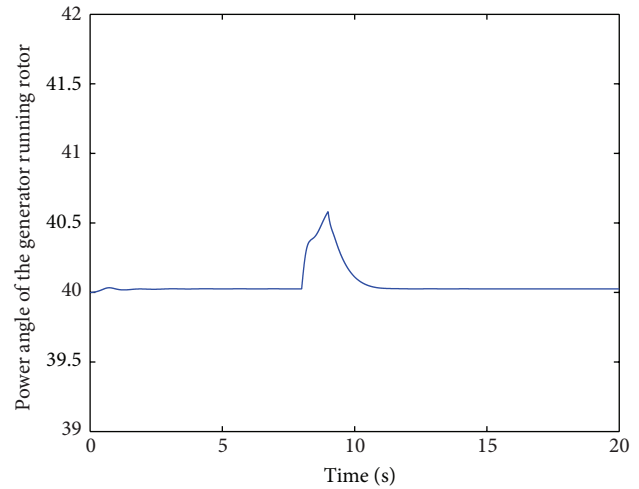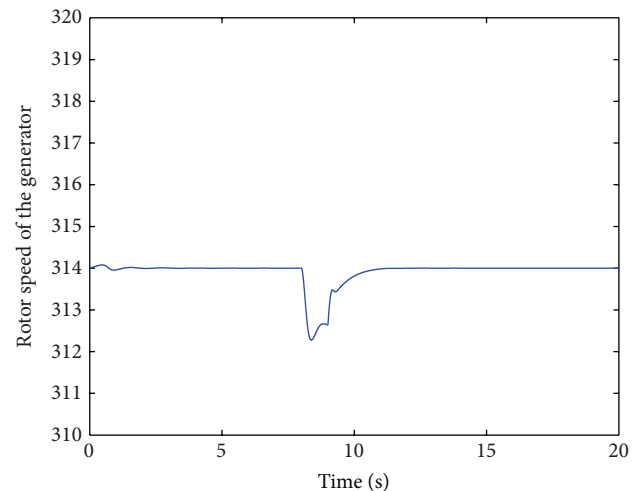
FIGURE 3: Tracking error and the performance function.

FIGURE 4: The actual control law u_f of power angle.

FIGURE 5: The actual voltage control law u'_B of access point voltage.

FIGURE 6: The rotor angle δ of generator.

FIGURE 7: The rotor speed ω of generator.

We suppose that three-phase short-circuit occurred on the terminal of the line at $t = 8$ s and eliminate the fault at $t = 9$ s; the simulation results are shown in Figures 3, 4, 5, 6, 7, 8, 9, 10, 11, 12, and 13. Figure 3 shows that, by introducing the error transformed function, the system can be stabilized promptly when it encountered some emergencies such as three-phase short-circuit which means that our control scheme makes the generator excitation control system have strong robustness. The tracking error of power angle can be prespecified by using the performance function $\varpi(t) = 0.65e^{-8t} + 0.002$. Figures 4 and 5 are actual control of power angle and actual voltage control law of the access point voltage, respectively. From Figure 6–Figure 8 we can know that all the states in the control system recover to their desired values in a short time by using our dynamic surface control
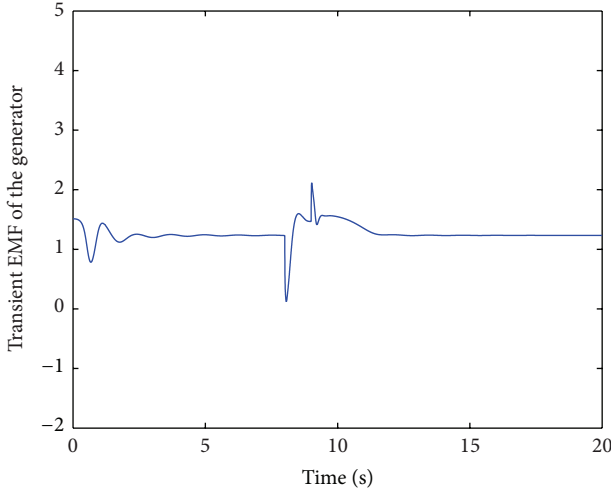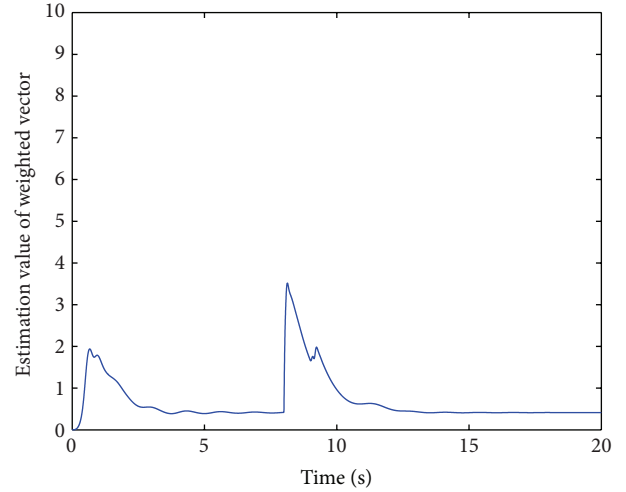
FIGURE 8: The transient EMF E'_q of the generator.

FIGURE 10: The estimated norm of the weighted vector $\hat{v}_3$, with $v_3^* = \|\theta_{\delta_3}^{*T}\|^2$.

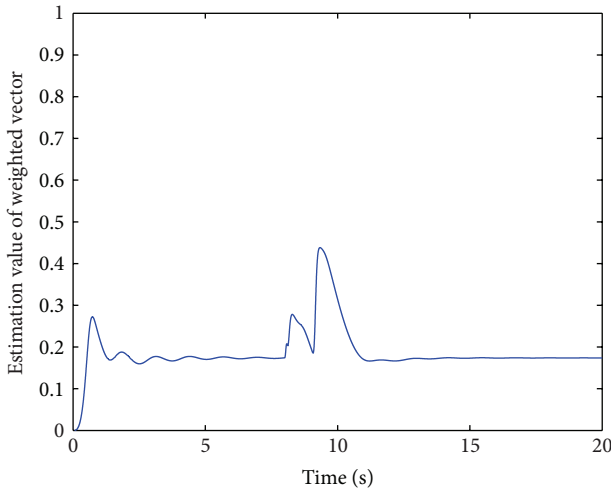
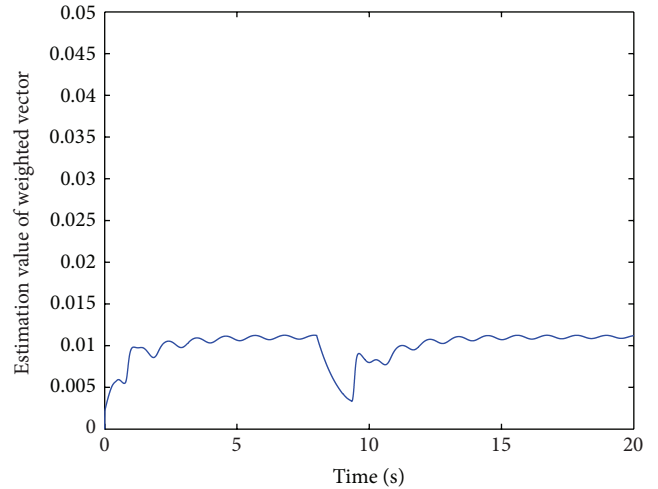FIGURE 9: The estimated norm of the weighted vector $\hat{v}_2$, with $v_2^* = \|\theta_{\delta_2}^{*T}\|^2$.

FIGURE 11: The estimated norm of the weighted vector $\hat{v}_4$, with $v_4^* = \|\theta_{\delta_4}^{*T}\|^2$.

scheme. Figure 9 to Figure 11 show the estimations of weight vector norm of the neural network. Figure 12 is the access point voltage increment $V_m - V_{\text{ref}}$, whose tracking process can also be arbitrarily prespecified by using performance function as that in Figure 3.

Remark 9. The controllers that have been proposed in [12, 13] are based on backstepping technique, which can cause the explosion of complicity problem that means the controller will become complex when the relative degree of the control system is high. Also, our novel neural network based adaptive dynamic surface controller is designed without doing any linearization to the excitation generator model. Therefore, the design procedures and the final control law are greatly simplified and the control accuracy is improved. Figure 13 has shown the comparison of the tracking error between our control scheme and backstepping control scheme.

6. Conclusion

This paper proposed a novel neural network and tracking error transformed function based on adaptive dynamic surface control scheme for the generator excitation control system which is equipped with SVC. In this scheme, both the designing procedures and the control law are simplified because it does not need to make any transformation to the excitation generator model. The prespecified tracking performance can be guaranteed by using the tracking error transformed function. The norm of the weighted vector of neural network is estimated which replaces the estimation of the weighted vector itself; therefore, the computational burden is greatly reduced. Also, the explosion of complicity problem inherent in the backstepping control can be eliminated. It is proved that the new scheme can make the system semiglobally uniformly ultimately bounded.
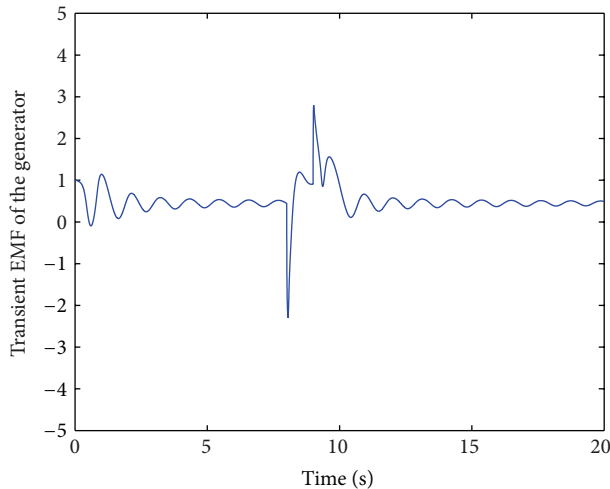
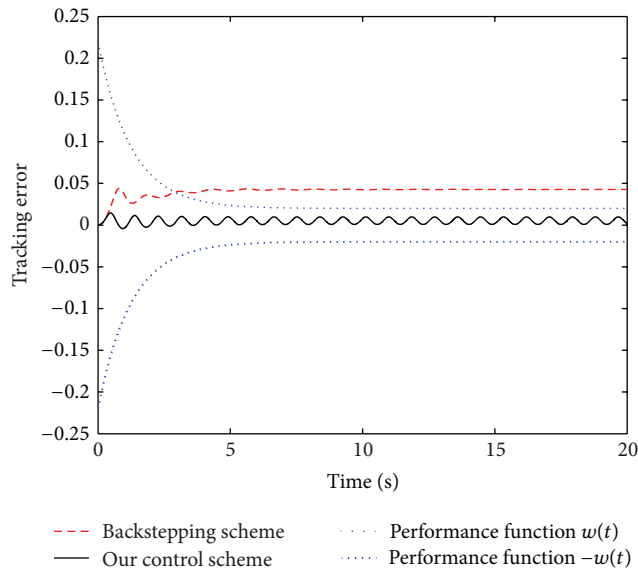FIGURE 12: The access point voltage increment $V_m - V_{ref}$.

FIGURE 13: The comparison of our NN based dynamic surface control scheme and backstepping.

Conflict of Interests

The authors declare that there is no conflict of interests regarding the publication of this paper.

Acknowledgments

References

[1] P. Kundur, *Power System Stability and Control*, China Electric Power Press, Beijing, China, 2002.

[2] A. J. Saavedra-Montes, J. M. Ramirez-Scarpetta, and O. P. Malik, "Methodology to estimate parameters of an excitation system based on experimental conditions," *Electric Power Systems Research*, vol. 81, no. 1, pp. 170–176, 2011.

[3] F. Zhu, H. Zhao, Z. Liu et al., "Effects of interconnected power grid on power system dynamic stability," *Proceedings of the CSEE*, vol. 27, no. 1, pp. 1–7.

[4] W. Ben and M. Zongyuan, "Giant synchronous generation-set's variable structure controller," *Proceedings of the EPSA*, vol. 10, no. 2, pp. 1–6, 1998.

[5] Y. Peihong, "The influence of excitation system to the stable operation of the power grid," Inner Mongolia University of Science and Technology, Inner Mongolia, China, 2008.

[6] H. Renmu, S. Feng, H. Dong et al., "The study of generator excitation system modeling and parameters estimation," *Power System Technology*, vol. 31, no. 14, pp. 62–67, 2007.

[7] Q. Liu, *The Stability of Powersystem and Excitation Control System*, China Electric Power Press, Beijing, China, 2007.

[8] K. Fregene and D. Kennedy, "Stabilizing control of a high-order generator model by adaptive feedback linearization," *IEEE Transactions on Energy Conversion*, vol. 18, no. 1, pp. 149–156, 2003.

[9] G. Fusco and M. Russo, "A nonlinear control of synchronous generator excitation for voltage regulation in power systems," in *Proceedings of the Mediterranean Conference on Control and Automation (MED '08)*, pp. 158–162, Ajaccio, France, June 2008.

[10] A. Colbia-Vega, J. de León-Morales, L. Fridman, O. Salas-Peña, and M. T. Mata-Jiménez, "Robust excitation control design using sliding-mode technique for multimachine power systems," *Electric Power Systems Research*, vol. 78, no. 9, pp. 1627–1634, 2008.

[11] L. Wan and Y. Chen, "Comprehensive nonlinear robust control for steam-valving and excitation system applying zero dynamic and variable structure control," *Proceedings of the Chinese Society of Electrical Engineering*, vol. 28, no. 13, pp. 26–32, 2008.

[12] H. A. Yousef, M. Hamdy, and M. Shafiq, "Flatness-based adaptive fuzzy output tracking excitation control for power system generators," *Journal of the Franklin Institute*, vol. 350, no. 8, pp. 2334–2353, 2013.

[13] F. Zhang and S. Zhu, "Adaptive excitation controller based on strong tracking filter," *Proceedings of the Chinese Society of Electrical Engineering*, vol. 25, no. 23, pp. 31–35, 2005.

[14] S. Mehraeen, S. Jagannathan, and M. L. Crow, "Power system stabilization using adaptive neural network-based dynamic surface control," *IEEE Transactions on Power Systems*, vol. 26, no. 2, pp. 669–680, 2011.

[15] X. Wang, *Adaptive Variable Structure Control of Nonlinear Power System*, Nanjing University of Science and Technology, Nanjing, China, 2011.

[16] L. Xiong, M. Xu, and S. Yuanzhang, "Nonlinear constant reactive power excitation control," *Electric Power Automation Equipment*, vol. 24, no. 5, pp. 1–4, 2004.

[17] Y. Wei, W. Wensheng, and H. Zhiming, "The Ddirect feedback linearization method for designing SSSC nonlinear control law," *Proceedings of the Chinese Society of Electrical Engineering*, vol. 23, no. 3, pp. 65–68, 2003.

[18] S. Zhou and X. Wang, "Direct feedback linearization based nonlinear excitation controller," *Proceedings of the Chinese Society of Electrical Engineering*, vol. 15, no. 4, pp. 281–288, 1995.

[19] B. Ren, S. S. Ge, C. Su, and T. H. Lee, "Adaptive neural control for a class of uncertain nonlinear systems in pure-feedback form with hysteresis input," *IEEE Transactions on Systems, Man, and Cybernetics B: Cybernetics*, vol. 39, no. 2, pp. 431–443, 2009.

[20] R. Sanne M and M. J. Mears, "Stable adaptive tracking of uncertainty systems using nonlinearly parameterized on-Line approximators," *IEEE Transactions on Neural Networks*, vol. 3, no. 6, pp. 837–863, 1992.

[21] C. P. Bechlioulis and G. A. Rovithakis, "Adaptive control with guaranteed transient and steady state tracking error bounds for strict feedback systems," *Automatica*, vol. 45, no. 2, pp. 532–538, 2009.

[22] C. P. Bechlioulis and G. A. Rovithakis, "Robust adaptive control of feedback linearizable MIMO nonlinear systems with prescribed performance," *IEEE Transactions on Automatic Control*, vol. 53, no. 9, pp. 2090–2099, 2008.

[23] W. Sun, H. Gao, and O. Kaynak, "Adaptive backstepping control for active suspension systems with hard constraints," *IEEE/ASME Transactions on Mechatronics*, vol. 18, no. 3, pp. 1072–1079, 2013.

[24] W. Sun, Z. Zhao, and H. Gao, "Saturated adaptive robust control for active suspension systems," *IEEE Transactions on Industrial Electronics*, vol. 60, no. 9, pp. 3889–3896, 2013.